Role of the Methoxy Groups in Cryptophanes for Complexation of Xenon. Conformational Selection Evidenced by 129 Xe-1 H NMR SPINOE Experiments

Patrick Berthault, Céline Boutin, Estelle Léonce, Erwann Jeanneau, Thierry Brotin

Role of the Methoxy Groups in Cryptophanes for Complexation of Xenon. Conformational Selection Evidenced by ^{129}Xe-^{1}H NMR SPINOE Experiments.

Patrick Berthault,*[b] Céline Boutin,[b] Estelle Léonce,[b] Erwann Jeanneau,[c] Thierry Brotin *[a]

Abstract: We report the laser-polarized ^{129}Xe and ^{1}H NMR spectra of a series of cryptophane derivatives that differ only by the number of methoxy groups attached on their benzene rings and the arrangement *syn* or *anti* of the linkers (compounds **6a-s**, **9a-s**, **12a-s**). All these compounds bind xenon even though the characteristic signal of the gas encapsulated in the cavity of the cage-molecule cannot be always detected. Interestingly, the exchange dynamics of xenon strongly depends on the degree of substitution and is different from that of the cryptophane derivatives studied previously. In solution, the ^{1}H NMR spectra of these derivatives show the presence of different conformations in a slow exchange regime that can be explained by a decrease of the flexibility of their skeleton. Thanks to ^{129}Xe-^{1}H dipolar cross-relaxation (SPINOE) spectra we demonstrate that a single conformation present in solution can bind xenon.

Introduction

Xenon is known to show good affinity for organic structures such as the hydrophobic pockets of proteins or hollow organic compounds capable of accommodating substrates in their cavities.[1-4] For instance, it has been reported that xenon presents a good affinity for cryptophane-A (**1**), a synthetic organic compound with a roughly spherical cavity.[5] Since this discovery, numerous xenon-cryptophane complexes have been thoroughly studied in organic or aqueous solution.[6] These supramolecular complexes also bring attention of the scientific community as they can be used for ^{129}Xe NMR-based biosensing applications.[7] The remarkable properties of these complexes mainly arise from the high receptiveness of the xenon nuclear spin, which is able to detect subtle changes in its surrounding environment.[8] Thus, when xenon is bound to a host molecule, the magnetic properties of its nucleus are modified resulting in a specific ^{129}Xe NMR signature for this complex. The possibility to modify the host structure in order to graft a biological site that can specifically recognize a biological target represents another advantage for these systems.[9]

From a more fundamental point of view, ^{129}Xe NMR spectroscopy appears as the tool of choice for studying cryptophane derivatives with small cavities. For instance, the xenon atom present within the cavity of cryptophane-A congeners shows a chemical shift significantly modified with respect to that of xenon present in the bulk. As an example, in 1,1,2,2-tetrachloroethane-d_2 the ^{129}Xe NMR spectrum of the Xe@cryptophane-A complex shows a chemical shift difference of 160 ppm between xenon in solution and xenon trapped into the cryptophane cavity.[5] The highly polarizable electron cloud of the xenon atom and the shielding of the six aromatic rings are responsible for this shift. Small changes in the structure of these derivatives can also have an impact on the physical properties of the complexes with xenon. For instance, a reduction of the volume of the cavity can modify both the association constant of the complex and the in-out exchange dynamics of xenon. As an example, the ^{129}Xe NMR spectrum of xenon with cryptophane-111, one of the smallest cryptophanes, gives rise to a very sharp signal at 30 ppm in 1,1,2,2-tetrachloroethane-d_2. This chemical shift differs significantly from the one obtained for the Xe@cryptophane-A complex. This complex is also characterized by a very high affinity constant, K = 10000 M^{-1} at 293 K.[10] A modified water-soluble cryptophane-111 also exhibits a remarkable xenon binding constant and an unusual downfield-shifted signal.[11] Even though numerous xenon@cryptophane complexes have been studied in the past, a prediction of the physical properties of the complexes (xenon chemical shift, in-out exchange dynamics, binding constant) remains difficult with these systems. Thus, to date it is difficult to establish a clear relationship between the chemical structure of the host molecule and the physical properties of the complexes. This is probably because these molecules show some flexibility. Thus, they can modify the conformation of their linkers to maximize their interaction with xenon. For instance, the ability of the cryptophane skeleton to adapt its conformation upon binding with xenon has been demonstrated by Pines and co-workers using SPINOE experiments.[12] They showed that cryptophane-A changes the conformation of its three O-CH_2-CH_2-O linkers upon encapsulation of xenon.

The study of new xenon@cryptophane derivatives is highly desired for a better understanding of the physical properties of these systems and specially to understand how structural modifications of the cryptophane scaffold can modify the physical properties of the complex. In this article, we report the study of xenon in interaction with several cryptophane-A congeners, whose structures are reported in Scheme 1. These molecules differ from cryptophane-A (**1**) by the number of methoxy substituents attached on the benzene rings or by the *syn* or *anti* arrangement of the three linkers connecting the two CTB units. For sake of simplicity the nomenclature of the new molecules used in this article refers to the number of methoxy substituents attached on the aromatic rings and the *anti* or *syn* arrangement of the linkers. For instance, cryptophanes **3a (2)** and **3s (3)** are molecules that possess only three methoxy substituents attached on the cryptophane scaffold. The subscripts **a** and **s** refer to the *anti* and *syn* arrangement of the three linkers, respectively. In other Articles these molecules have been called cryptophane-C and D (Collet's nomenclature), respectively. Similarly, compounds **4** and **5** that contain six methoxy on the same CTB unit, are noted in the text compounds **6a** and **6s**, respectively. Using the same nomenclature, compounds **6** and **7** are noted **9a** and **9s**, respectively, whereas compounds **8** and **9** that possess the highest degree of substitution with twelve methoxy substituents attached on the six aromatic rings are noted **12a** and **12s**, respectively.

With the exception of compound **12s,** these cryptophanes are chiral molecules. The chiroptical properties of these derivatives have been thoroughly described in a recent Article.[13] Cryptophane **12a** has D_3-symmetry and the chirality of this compound originates from the helical arrangement of the three linkers. Compound **12s** has a plane of symmetry and is therefore achiral (C_{3h} symmetry). Interestingly, it is noteworthy that the *syn*-stereoisomer of cryptophane-A has never been isolated. Thus, compound **12s** is of high interest in this study. Molecules **6a - 6s** and **9a - 9s** possess a lower degree of substitution than compounds **12a** and **12s**, with six and nine methoxy groups, respectively (see Scheme 1). The synthesis of new

[a] T.Brotin
Laboratoire de Chimie de L'ENS LYON (UMR 5182)
Ecole Normale Supérieure de Lyon
46, Allée D'Italie
69364 Lyon cedex 07, France
E-mail: thierry.brotin@ens-lyon.fr

[b] P. Berthault, C. Boutin, E. Léonce
NIMBE, CEA, CNRS
Université de Paris Saclay, CEA Saclay
91191 Gif-sur-Yvette, France
E-mail: patrick.berthault@cea.fr

[c] E. Jeanneau
Centre de Diffractométrie Henri Longchambon
Université de Lyon 1, 5 rue la Doua
69100 Villeurbanne, France

Supporting Information for this article is given at the end of the document.

derivatives **6a** and **6s** is described for the first time in this Article. The introduction of additional methoxy groups on the cryptophane backbone and the *syn* or *anti* arrangement of the three O-CH_2-CH_2-O linkers are expected to modify the physical properties of the xenon@cryptophane complexes. For instance, the introduction of additional electron-donating substituents on the cryptophane scaffold should have an impact on the caged xenon chemical shift.[14] In addition, the *anti* or *syn* arrangement of the linkers should modify the in-out exchange dynamics of xenon.

In this Article, we report both their ^{1}H NMR and their hyperpolarized ^{129}Xe NMR spectra. The spin-hyperpolarization technique is a powerful tool that allows a gain in sensitivity by a factor 10^4-10^5 thus enabling to record ^{129}Xe NMR spectra in few seconds with excellent signal to noise ratio. We also report the ^{129}Xe-^{1}H dipolar cross-relaxation (SPINOE) spectra of these complexes. The results obtained with compounds **6a-s**, **9a-s** and **12a-s** are then compared with those previously obtained with the Xe@**1,** Xe@**3a** and Xe@**3s** complexes. Our results shed light on the role of the substituents in the variation of the physical properties of these complexes. Thanks to ^{129}Xe-^{1}H SPINOE spectroscopy, we show that a conformational selection occurs upon encapsulation with xenon.

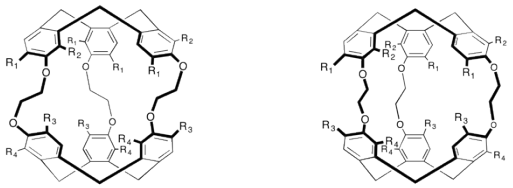

1 : R_1 = OMe; R_2 = H; R_3 = OMe; R_4 = H (cryptophane-A)
2 : R_1 = OMe; R_2 = H; R_3 = H; R_4 = H
3 : R_1 = OMe; R_2 = H; R_3 = H; R_4 = H
4 : R_1 = OMe; R_2 = OMe; R_3 = H; R_4 = H
5 : R_1 = OMe; R_2 = OMe; R_3 = H; R_4 = H
6 : R_1 = OMe; R_2 = OMe; R_3 = OMe; R_4 = H
7 : R_1 = OMe; R_2 = OMe; R_3 = OMe; R_4 = H
8 : R_1 = OMe; R_2 = OMe; R_3 = OMe; R_4 = OMe
9 : R_1 = OMe; R_2 = OMe; R_3 = OMe; R_4 =OMe

Scheme 1. Chemical structures of the *anti*-cryptophanes **1**, **2** (3a), **4** (6a), **6** (9a), **8** (12a) and the *syn*-diastereomers **3** (3s), **5** (6s), **7** (9s) and **9** (12s).

Results and Discussion

Synthesis and characterization of compounds 6-12: compounds **9a-s** and **12a-s** (Scheme 1) have been prepared according to a known procedure.[15] New derivatives **6a** and **6s** have been prepared using a similar strategy (see Scheme 2). The known 10,15-dihydro-5*H*-Tribenzo[*a*,*d*,*g*]cyclononene-2,7,12-triol, **10** is allowed to react with 2*H*-Pyran, tetrahydro-2-[[4-(2-iodoethoxy)-3,5-dimethoxyphenyl] methoxy]- **11** in the presence of cesium carbonate in DMF to give rise to the cryptophane precursor **12** in good yield (72 %).[15] The second ring closing reaction is then performed at 55°C in a mixture of formic acid and $CHCl_3$. This gives rise to a crude product that contains compounds **6a** and **6s** in similar proportion. It is noteworthy that both compounds show very similar retention time on silica gel. Compound **6s** is eluted first on silica gel and is isolated in 29% yield with high purity. The purification of the second diastereomer **6a** is more difficult and requires additional purification steps as described in the experimental section. Compound **4** (**6a**) is obtained with the same yield (29%). Compounds **6a** and **6s** have been fully characterized by ^{1}H, ^{13}C NMR spectroscopy and HRMS. ^{1}H NMR and ^{13}C NMR spectra of compound **6a** and **6s** are given in Supporting Information (Figures S1-S4 in the Supporting Information).

X-Ray structures of compounds 6a and 6s: Single X-ray quality crystals have been obtained for both diastereomers **6a** and **6s** in a mixture of chloroform and ethanol. Their crystallographic data of are summarized in Supporting Information (Table S5 in the Supporting Information). Both compounds crystallize in a $P2_{1/n}$ space group. For the two structures four molecules are present in the lattice. One $CHCl_3$ molecule is present in the X-ray structure of **6a** and another $CHCl_3$ molecule is present outside the cavity (Figure S6 in the Supporting Information). The refined structure of **6a** also reveals residual electronic density within the cavity that could correspond to a statistical occupation of half the cryptophane molecules by a $CHCl_3$ molecule. The refined structure of **6s** shows two $CHCl_3$ molecules located outside the cavity and another $CHCl_3$ molecule present within the cavity of **6s** (Figure S7 in the Supporting Information). The refined X-ray structure of compound **6a** shows that some disorder is present. Indeed, as often observed in X-ray structures of the cryptophane derivatives, the three linkers can adopt different conformations. While the *trans-trans-trans* (*ttt*) and the *trans-trans-gauche* conformations are present in the X-ray structure of **6a**, the X-ray structure of **6s** does not show any disorder and the three linkers have an *all-trans* (*ttt*) conformation. The non-helical structure of **6s** (C_3 symmetry) and the *ttt* conformation give rise to a large inner cavity, which has been estimated to be 147 Å^3. By contrast the mean value calculated for the inner cavity of **6a** is 91 Å^3. For both compounds, the six methoxy groups show different orientations. Three methoxy groups are located in the plane of the bridges, whereas the three others are located out of the plane of the three benzene rings (cif files). This orientation is consistent with the X-ray structures of cryptophane-A (**1**) and compounds **9a**, **9s**, **12a**, **12s** previously reported by our group.[15,17] For instance, the X-ray structure of the cryptophane-A derivative shows that the methoxy groups are in the plane of the benzene rings. In contrast, the introduction of additional methoxy substituents results in a change of orientation of these groups since they are located out of the plane of the benzene rings. A steric hindrance can explain this difference of orientation.

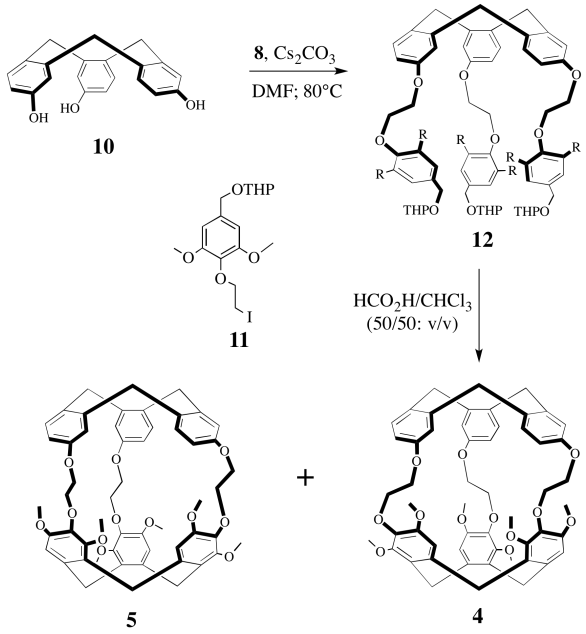

Scheme 2. synthesis of the cryptophane diastereomers *anti*-**6a** (**4**) and *syn*-**6s** (**5**).

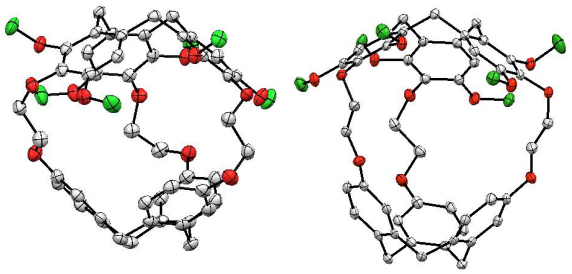

Figure 1 X-ray structures of **6a-(4**; left**)** (disordered parts have been omitted for clarity) and **6s-(5**; right**)** diastereomers. In both structures the $CHCl_3$ molecule present inside the cavity as well as the hydrogen atoms have been removed for clarity.

^{129}Xe NMR Spectroscopy: For this study, 1,1,2,2-tetrachloroethane-d_2 has been chosen as a solvent because it is not supposed to enter the cavity of these cryptophanes and therefore is not a competitor for

xenon. In these experiments, xenon gas is added after degassing the organic solutions that contain the different cryptophane derivatives. From the one-scan hyperpolarized ^{129}Xe NMR spectra of the compounds **6a**, **6s**, **9a**, **9s**, **12a** and **12s** recorded in the same conditions (Figure 2), it is worth noting that the xenon in-out exchange rate exhibits large variation depending on the nature of the cryptophane skeleton. A large peak at 225 ppm that corresponds to xenon free in 1,1,2,2-tetrachloroethane-d_2 can be clearly identified in all cases. A second up-field shifted signal of weaker intensity is sometimes located, thus revealing directly the caged xenon environment. For the *anti* cryptophane **6a** at sub-millimolar concentration, in our experimental conditions, a fast exchange situation is observed (or no xenon encapsulation). In contrast, for the compounds **9a** and **12a** a slow exchange is encountered at sub-millimolar concentration and under the same experimental conditions, and the caged xenon signal is shifted towards higher field when the number of OCH_3 groups increases. Somewhat counter intuitively a broader line is observed for Xe@**12a** than for Xe@**9a**, indicating a faster xenon in-out exchange. On the other hand, compounds **6s**, **9s** and **12s** do not show any signal corresponding to the complexes. However, it can be mentioned that the ^{129}Xe NMR spectrum of compound **6s** shows a broadening of the free xenon signal suggesting that encapsulation of xenon occurs under not so fast exchange conditions. The xenon in-out exchange is likely to be slowed down by the six methoxy groups on one CTB unit. For compounds **9s** and **12s**, the free xenon exhibits sharp signals. Consequently, the ability of the xenon atom to enter the cavity of compounds **9s** and **12s** is questionable.

If one considers that the xenon in-out exchange is strongly dependent upon the *anti* or *syn* arrangement of the three linkers (slow exchange at the NMR scale for the anti-cryptophanes, fast exchange for the syn-cryptophanes), the two exceptions are cryptophanes **6a** and **6s**. Cryptophane **6a** reveals a behavior that is different from what is observed with cryptophane-A (**1**) and cryptophane **3a** (figure S10 in the Supporting Information). For instance, it has been reported that complexation of xenon with **3a** – whatever the xenon/cryptophane concentration ratio - occurs under a slow exchange regime. For cryptophane **6s**, xenon exhibits an intermediate exchange. This can be compared to the behavior of diastereomer **3s** that shows a fast exchange regime at 293 K but for which a signal characteristic of the complex is observed at lower temperature.[18] A common cryptophane scaffold constituted by only one highly methoxylated CTB seems to be responsible of this effect.

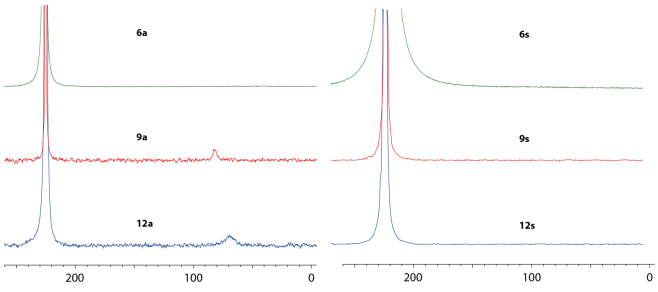

Figure 2. One-scan ^{129}Xe NMR spectra of the samples of **6 (a** and **s), 9 (a** and **s), 12 (a** and **s).** The subscripts a and s refer to *anti* and *syn* arrangement of the linkers. Spectra have been recorded at 11.74 T and 293 K. Each sample contained 0.3 +- 0.03 mg of cryptophane (0.4 - 0.5 mM) in 600 µL of 1,1,2,2-tetrachloroethane-d_2 and *ca.* 10 mg of xenon (representing a concentration of ca. 100 mM).

^{1}H NMR spectra of the cryptophane derivatives: the difference observed with compounds **6a-s**, **9a-s** and **12a-s** in the presence of xenon prompted us to examine more carefully their ^{1}H NMR spectra. We thus report in this Article the ^{1}H NMR spectra of compounds **6a-s**, **9a-s** and **12a-s** under degassed solution and in the presence of xenon. We also report the ^{129}Xe-^{1}H cross-relaxation (SPINOE) experiments.[19] These experiments are very useful to establish whether xenon enters or not the cavities of compounds **6a-s**, **9a-s** and **12a-s** since the ^{129}Xe-^{1}H cross-relaxation only occurs at very short distance. The lack of solvent peak (6.0 ppm) in the SPINOE spectra of compounds **6a-s**, **9a-s** and **12a-s** is a good indicator that these experiments have been successfully performed.

As an example, Fig. 3 displays the ^{1}H NMR spectra of cryptophanes **12a** and **12s** in degassed solution (Fig. 3a and 3b) and after introduction of xenon into the solution (Fig 3c and 3d). Fig. 3e and 3f display the ^{129}Xe NMR SPINOE spectra of compound **12a** and **12s**, respectively. Degassing the solution before introducing xenon is a mandatory step to avoid fast ^{129}Xe relaxation by paramagnetic molecular oxygen and to avoid possible competing binding with other dissolved gases. Interestingly, we notice that introduction of xenon into the solutions deeply modifies the ^{1}H NMR spectra: important changes occur for both the *anti* and *syn* cryptophanes. For instance, for the degassed solution of **12a**, the aromatic part of the proton spectrum shows two signals with very different intensities. For the sample in the presence of xenon this region now reveals a unique peak that corresponds to the minor NMR signal observed in the case of the degassed solution. The axial protons H_a of the CTB units (4.2 ppm) are also strongly affected by the presence of xenon in solution. For instance, we can notice on Figure 3a that the H_a signals originally observed for the degassed solution have been replaced by another up-field shifted doublet. It is noteworthy that signals characteristic of the three linkers (dashed line) are also strongly affected by the presence or not of xenon inside the solution. Indeed, the two signals initially observed at 4.14 ppm and 3.94 ppm are replaced by an intense multiplet located at 3.99 ppm. The ^{129}Xe NMR SPINOE sub-spectrum of **12a** reveals a simplified spectrum where only the protons that are in close proximity to xenon appear. Dealing with the aromatic protons, for **12a**, no change is observable compared to the ^{1}H NMR spectrum of the solution with xenon. In contrast, the aliphatic part is strongly simplified (in particular as expected the axial proton signals of the CTB are strongly attenuated).

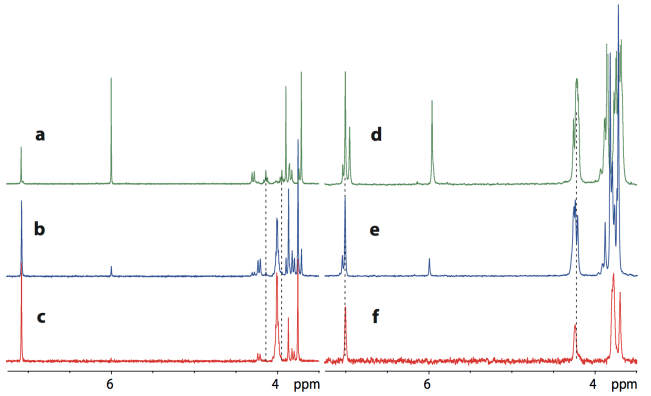

Figure 3. Comparison of the ^{1}H NMR spectra for compounds **12a** (left) and **12s** (right). The samples were constituted by 0.3 mg of cryptophane **12a** in 600 µL of 1,1,2,2-tetrachloroethane-d2 and 0.3 mg of cryptophane **12s** in 600 µL of 1,1,2,2-tetrachloroethane-d2. From top to bottom, the green spectra were recorded with the degassed solution, the blue ones after introduction of xenon into solution, and the red ones correspond to the results of the SPINOE experiments obtained with the sequence of ref. [20].

The changes observed between the ^{1}H spectra of the degassed solution, of the solution in the presence of xenon and of the SPINOE (Fig. 3a, 3b and 3c) suggest that the introduction of xenon into the solution has a strong impact on the conformation of the three linkers. A comparison between these spectra indicates that compound **12a** has to change the conformation of the three linkers to accommodate the xenon atom. This effect can clearly be evidenced in the aliphatic region of the spectrum.

For compound **12s**, the spectral changes between the three spectra are even more important. The degassed solution of **12s** exhibits a ^{1}H spectrum with numerous signals present in the aromatic and aliphatic regions. It reveals that compound **12s** possesses at least three different conformations of the bridges in slow exchange regime. This is supported by the presence of three well-resolved signals in the aromatic part of the spectrum. The addition of xenon into the solution results in a simplification of the ^{1}H NMR spectrum and two NMR signals with close intensities are observed in the aromatic part. The aliphatic part of the ^{1}H NMR spectrum is also affected by the presence of xenon. However, this spectral region is not very informative due to the strong overlapping of the different signals present in that region.

From the single ^{129}Xe NMR spectrum, there was no evidence of xenon encapsulation by cryptophane **12s**. But the presence of xenon

inside the cavity of **12s** could be ascertained from its ^{129}Xe-^{1}H SPINOE spectrum, revealing some well-defined ^{1}H signals. For instance, the aromatic region reveals a single NMR peak, and a strong simplification in the aliphatic part of the spectrum is also clearly observed. Combined together these results show that compound **12s** can easily adopt different conformations in solution depending on the experimental conditions. The presence of these conformations seems to be favored in the absence of guest inside the cavity of **12s**. Upon addition of xenon, several conformations are still present in solution but only one conformation seems to be able to bind efficiently xenon.

The ^{1}H NMR spectra of derivatives **9a-s and 6a-s** (Figures. S8 and S9 in the Supporting Information) that possess two CTB units with a different degree of substitution, also result in important spectral changes upon addition of xenon. These compounds possess a lower symmetry (C_3) than cryptophanes **12a** (D_3) or **12s** (C_{3h}). Their corresponding ^{1}H NMR spectra are therefore more complicated to interpret due to the presence of additional signals in the aromatic region of the ^{1}H NMR spectrum. The ^{1}H NMR spectrum of a degassed solution of **9a** shows several signals of with different intensities in the aromatic region (Figure S9a in the Supporting Information). Considering the molecular symmetry of **9a** and the relative intensities of the signals, we expect three signals in the aromatic region. However five distinct peaks appear in this region, suggesting the presence of several conformations in a slow exchange regime. This is also supported by the presence of several doublets in the aliphatic region of the spectrum for protons H_a and H_e. As observed for compounds **12a** and **12s**, for **9a** a simplification of the ^{1}H NMR spectrum is observed after introduction of xenon into the solution. For instance, the aromatic region of the Xe@**9a** complex is dominated by two intense signals (two protons of **9a** resonate at the same frequency). Three other signals of much lower intensity are also present in this region and indicate the presence of another conformation in minor proportion. A simplification of the ^{1}H NMR spectrum of **9a** in the aliphatic region is also observed (Figure S8b in the Supporting Information). The differences observed between these two spectra suggest that a strong rearrangement of the linkers takes place upon addition of xenon. The ^{129}Xe-^{1}H SPINOE of **9a** shows a simplified spectrum with respect to that of the Xe@**9a** complex. Once again, this simplification is clearly visible in the aromatic part of the spectrum since only two intense signals are now visible. Spectral changes are also observed in the aliphatic part.

As observed for its diastereomer, compound **9s** also shows important spectral modifications upon addition of xenon into the solution. For instance, the ^{1}H NMR spectrum of the degassed solution of **9s** (Figure S8d in the Supporting Information) shows the presence of at least two major forms in ca. 1:2 ratio and an additional minor form. This situation where two forms dominate, is different from that obtained for **9a**, and can be interpreted considering the *syn* arrangement of the linker. Upon addition of xenon, this ratio is reversed, revealing a clear induction effect of xenon. Interestingly, the ^{129}Xe-^{1}H SPINOE spectrum of **9s** shows a simplified spectrum suggesting that a cryptophane with a unique conformation of the linkers can effectively accommodate xenon. Once again, as mentioned for compound **12s**, the ^{129}Xe-^{1}H SPINOE technique is a valuable tool to discriminate between the different conformations that bind or not xenon. In the case of compound **9s** it can be clearly established that a single conformation of the bridges can accommodate xenon in solution, even though several conformations in a slow exchange regime can be detected on the ^{1}H NMR spectrum of **9s**.

Among the different compounds studied in this Article, compound **6a** and its diastereomer **6s** have the lowest degree of substitution. The ^{1}H NMR spectrum of a degassed solution of **6a** (figure S9a in the Supporting Information) is very simple; the presence of 4 aromatic signals is indicative of a single conformation. This is supported by the presence of only two sets of signals for the H_a and H_e protons. At first glance, this result may appear surprising considering that compounds with a higher degree of substitution showed several conformations in slow exchange. However, it can be interpreted considering the higher flexibility of compound **6a** in which one of the two CTB unit is devoid of substituents. Upon addition of xenon, only slight modifications of the spectrum occur more specifically in the aliphatic region of the spectrum. The ^{129}Xe -^{1}H SPINOE sub-spectrum of **6a** gives the same signals except the axial and equatorial methylene protons. Consequently, compound **6a** exhibits in solution a single conformation of the linkers whatever the xenon concentration (from 10 mM to 100 mM, data not shown). This conformation is able to accommodate xenon, even though no specific ^{129}Xe NMR signal for the complex is detected at 293K. The absence of spectral changes between these three spectra could indicate that the cavity size is too large to be modified upon xenon encapsulation. With compound **6s** a different situation occurs: the aromatic region of the ^{1}H spectrum for the degassed sample exhibits two sets of signals (Figure. S9d in the Supporting Information). These two conformations are present in a similar proportion but the addition of xenon (Figure S9e in the Supporting Information) modifies their relative proportion, and the SPINOE sub-spectrum indicates a unique conformation able to accommodate xenon (Figure. S9f in the Supporting Information).

The helical arrangement of the linkers of the *anti*-cryptophanes is expected to give them more flexibility upon binding of guest molecules than *syn*-cryptophanes. It is surprising to observe that compound **6s** can modify its conformation to interact with xenon, whereas the ^{1}H NMR spectrum of its diastereomer **6a** remains unchanged. The ^{129}Xe-^{1}H SPINOE spectrum of **6s** (figure S9f in the Supporting Information) shows a simplification of the spectrum indicating that a single conformation can accommodate xenon.

The NMR experiments performed with compounds **3a-s**, **6a-s**, **9a-s** and **12a-s** lead to conclusions that may seem counter-intuitive. Indeed, the study of these compounds reveals that a correlation between the degree of substitution of the CTB units and the in-out exchange dynamics of xenon cannot be clearly established as initially expected. Similarly, a correlation between the arrangement *syn* or *anti* of the linkers and the exchange dynamics of xenon is not direct. Consequently, the in-out exchange dynamics of xenon with these derivatives cannot be explained solely on considerations based on the cavity size of the host molecules and the steric hindrance induced by the presence of the additional methoxy groups. Other factors must be involved to interpret these results. The presence of numerous conformational forms observed for the majority of these derivatives and the ability of these compounds to change the conformation of their linkers give us a clue. The ^{1}H NMR spectra of these compounds reveal that the linkers can adopt several conformations (trans or gauche) in solution. Importantly, these conformations are in a slow exchange regime. This is attested by the presence of distinct signals in the aromatic part of these compounds. On the other hand, the ^{129}Xe - ^{1}H SPINOE spectra of compounds **6a**-**6s**, **9a**-**9s** and **12a**-**12s** show a clear simplification with respect to their ^{1}H NMR spectra. Thus, these experiments demonstrate without exception that all the derivatives studied in this article bind xenon, even though a ^{129}Xe NMR signal characteristic of the complexes cannot be always detected. The ^{129}Xe - ^{1}H SPINOE spectra also indicate that a single conformation, among those detected by ^{1}H NMR spectroscopy, can effectively accommodate xenon. The presence of different conformations of the linkers, even after adding xenon into the solution, seems to be a consequence of the presence of the additional methoxy groups grafted on the CTB units. These substituents rigidify the cryptophane scaffold and constrain the linkers to adopt different conformations. This assumption is supported by the study of the ^{1}H NMR spectra of **3a** and **3s** (Figure S11 in the Supporting Information) that reveal a single conformation for the degassed and gassed samples.

In the case of compounds **6s**, **9a-9s** and **12a-12s** these different conformations are in a slow exchange regime. The *anti* derivatives **9a** and **12a**, thanks to the helical arrangement of their linkers are more flexible and they can more easily modify the conformation of their linkers to accommodate xenon. In contrast, the *syn* arrangement (compounds **6s**, **9s** and **12s**) of the linkers seems detrimental and several conformations of the linkers are still present even after introducing xenon.

Interestingly, these results show that cryptophane derivatives with similar linkers can exhibit very different physical properties in the presence of xenon. Changing the nature of the substituents attached on the cryptophane skeleton appears to be a simple way to change drastically the in-out exchange dynamics of xenon. However, the substituents effect on the exchange dynamics of xenon is difficult to predict. It is worth-mentioning that these considerations do not take into account interactions that could eventually take place between solvent molecules and the host molecules. Interactions are probably more important in the case of compounds **6a** and **6s** considering the

larger apertures observed for these two compounds. Molecular dynamics calculations of the complexes using an explicit solvation model would be a valuable tool to interpret these data. Such theoretical approach appears is very challenging considering the large size of these molecules and the number of solvent molecules needed for the calculations.

Conclusions

We report a study of the Xe@**6a-s, 9a-s** and **12a-s** complexes by ^{1}H NMR and ^{129}Xe NMR spectroscopy. These compounds differ from their congeners **1**-**3** by the number of methoxy substituents attached on the cryptophane-222 skeleton and the arrangement *syn* or *anti* of the linkers. We show that introduction of additional methoxy groups on the cryptophane backbone has a strong impact on the in-out exchange dynamics of xenon, whereas the lengths of the linkers are the same. Among this series, two cryptophanes have an unexpected behavior. Compound **6a** is the only *anti*-cryptophane in which xenon is in fast exchange on the ^{129}Xe NMR spectrum, **6s** is the only *syn*-cryptophane in which xenon displays an intermediate exchange regime, as evidenced by the broadening of the low-field signal. However for these two compounds we cannot exclude a contribution of the solvent molecules to explain these results.

The introduction of methoxy substituents positioned from each side of the linker rigidifies the cryptophane-222 scaffold. Thus, in solution these compounds show several conformations of their bridges in slow exchange dynamics. This effect seems more pronounced with the *syn* derivatives, which are more rigid. Addition of xenon into the solution modifies the relative distribution of these conformations. The *anti* derivatives having a higher flexibility show a major conformation for the linkers after introduction of xenon. In contrast, the ^{1}H NMR spectra of the *syn* derivatives show several conformations in slow exchange even after introduction of xenon. The ^{129}Xe - ^{1}H SPINOE spectra provide additional information and are valuable to distinguish the different conformations that effectively accommodate xenon that the other ones that do not. In our case, the ^{129}Xe - ^{1}H SPINOE spectra reveal that only a single conformational present in solution can bind xenon.

Combined together these results demonstrate that cryptophane derivatives possessing identical linkers can possess very different properties towards xenon encapsulation. This effect can possibly be exploited for ^{129}Xe NMR-based biosensing application. It would be a way to tune the in-out exchange dynamics that play a key role for sensitive NMR detection, helped in that by recent solutions from the literature based on quantitative analysis of saturation-transfer experiments.[21]

Experimental Section

Mass spectra (HRMS LSIMS) were performed by the Centre de Spectrométrie de Masse, University of Lyon, on a Thermo-Finnigan MAT 95XL spectrometer. ^{1}H and ^{13}C NMR spectra were recorded on a 300 MHz NMR spectrometer at 300 and 72 MHz, respectively. Chemical shifts are in δ values from Me_4Si (^{1}H, ^{13}C). Column chromatographic separations were carried out over Merck silica gel 60 (0.040-0.063 mm). Analytical thin layer chromatography (TLC) was performed on Merck silica gel TLC plates F-254. The solvents were distilled prior to use: DMF and CH_2Cl_2 from CaH_2, THF from Na/benzophenone and pyridine from KOH.

Synthesis of compound 12. Iodo derivative **11** (2.11 g, 6.1 mmol) was added in one portion to a stirred solution of 10,15-Dihydro-5H-tribenzo[a,d,g][9]annulene-2,7,12-triol **7** (0.58 g, 1.82 mmol), cesium carbonate (1.98 g, 6.1 mmol) in DMF (35 mL). The mixture was stirred overnight at 80°C under an argon atmosphere. The mixture was poured in water and the product was extracted four times with AcOEt. The combined organic layers were then washed twice with brine and dried over Na_2SO_4. Filtration and evaporation of the solvent under reduced pressure to give yellow oil. The product was then purified on silica gel (eluent: AcOEt/Petroleum Ether: 50/50 then 75/25). The second spot was collected. The solvent was evaporated under reduced pressure to give rise to an oily product. Compound **12** was obtained as a white glassy product (1.58 g; 72 %) was then obtained by removing trace of solvent with the vacuum line. ^{1}H NMR (300 MHz, $CDCl_3$) δ 7.21 (3 H, d, *J* = 8.5 Hz), 6.89 (3 H, d, *J* = 2.7 Hz), 6.61 (3 H, dd, *J* = 8.5 Hz, J = 2.7 Hz), 6.55 (s, 6 H), 4.72 (3 H, d, *J* = 13.5 Hz), 4.69 (3 H, d, *J* = 11.5 Hz), 4.68 (3 H, m), 4.41 (3 H, d, *J* = 11.5 Hz), 4.30 - 4.10 (12 H, m), 3.90 (3 H, m), 3.74 (18 H, m), 3.59 (3 H, d, *J* = 13.5 Hz), 3.52 (3 H, m), 1.90 – 1.50 (18 H, m). ^{13}C NMR (75.475 MHz, $CDCl_3$, 25°C) δ 157.5 (3C), 153.3 (3C), 141.0 (3C), 136.1 (3C), 134.0 (3C), 131.6 (3C), 131.0 (3C), 116.2 (3C), 112.7 (3C), 104.9 (3C), 97.8 (3C), 71.2 (3C), 69.1 (3C), 66.9 (3C), 62.3 (3C), 56.0 (3C), 36.6 (3C), 30.6 (3C), 25.4 (3C), 19.5 (3C). HRMS (ESI) calcd for $C_{69}H_{84}O_{18}Na$ [M+Na$^+$], 1223.5550 found 1223.5503.

Synthesis of cryptophanes 4 (6a) and 5 (6s). In a 1000 mL round bottom flask, formic acid (300 mL) was added in one portion to a solution of cryptophane precursor **12** (0.55 g, 0.46 mmol) dissolved in chloroform (300 mL). The solution was stirred for 5 hours at 55°C. The solvents were removed under reduced pressure. Then $CHCl_3$ (100 mL) was added and the solvent was removed under reduced pressure. This procedure was repeated three times in order to remove traces of formic acid *via* azeotropic distillation. The crude product was then purified on silica gel (eluent: CH_2Cl_2/Acetone – 90/10) to give rise to a white glassy product (0.58 g). This product contains the two cryptophanes anti-**4 (6a)** and syn-**5 (6s)** in the same amount. A second column chromatography (eluent: CH_2Cl_2/Acetone – 99/01) allows the separation give rise to the pure syn-**5 (6s)** derivative (0.12 g; 29 %). This compound was then recrystallized in a mixture of $CHCl_3$ and EtOH. Compound **6**: ^{1}H NMR (300 MHz, $CDCl_3$) δ 7.11 (3H, s), 7.07 (3H, d, *J* = 8,7 Hz), 6.67 (3H, d, *J* = 2,4 Hz), 6.55 (3H, dd, *J* = 2,4 Hz, *J* = 8.7 Hz), 4.58 (3H, d, *J* = 13,5 Hz), 4.28 (3H, d, *J* = 13,5 Hz), 4.35 – 4.25 (3H, m), 4.25 – 4.10 (3H, m), 4.10 – 3.95 (3H, m), 3.91 (9 H, s), 3.87 (3H, d, *J* = 13,5 Hz), 3.73 (9H, s), 3.60 – 3.50 (3H, m), 3.46 (3H, d, *J* = 13,5 Hz). ^{13}C NMR (75.475 MHz, $CDCl_3$, 25°C) δ 157.14 (3C), 152.03 (3C), 151.31 (3C), 140.7 (3C), 139.1 (3C), 136.5 (3C), 132.1 (3C), 130.6 (3C), 125.3 (3C), 118.4 (3C), 113.1 (3C), 110.5 (3C), 69.8 (3C), 65.8 (3C), 60.2 (3C), 55.7 (3C), 36.0 (3C), 30.0 (3C). HRMS (ESI) calcd for $C_{54}H_{55}O_{12}$ [M$^+$], 895,3688 found 895,3674.

This product was then followed by compound **4 (6a)**, still contaminated by the presence of a small amount of compound 5 (**6s)**. Another column chromatography on silica gel (eluent: CH_2Cl_2/Acetone – 99/01) gives rise to the pure diastereomer **4** (0.12 g; 29 %). This product was then recrystallized in a mixture of $CHCl_3$ and EtOH. ^{1}H NMR (300 MHz, $CDCl_3$) δ 7.08 (3H, d, J = 8.3 Hz), 7.05 (3H, s), 6.74 (3H, d, *J* = 2.4 Hz), 6.39 (3H, dd, *J* = 2,4 Hz, *J* = 8.3 Hz), 4.62 (3H, d, *J* = 13,5 Hz), 4.28 (3H, d, *J* = 13,5 Hz), 4,2 – 4,0 (12 H, m), 3.85 (9H, s), 3.83 (3H, d, *J* = 13.5 Hz), 3,72 (3H, s), 3.49 (3H, d, *J* = 13.5 Hz). ^{13}C NMR (75.475 MHz, $CDCl_3$, 25°C) δ 157.6 (3C), 151.1 (3C), 150.8 (3C), 141.0 (3C), 139.4 (3C), 135.6 (3C), 132.6 (3C), 130.7 (3C), 125.4 (3C), 119.1 (3C), 115.5 (3C), 110.8 (3C), 70.1 (3C), 68.2 (3C), 60.1 (3C), 55.6 (3C), 36.3 (3C), 29.9 (3C). HRMS (ESI) calcd for $C_{54}H_{55}O_{12}$ [M$^+$], 895.3688 found 895.3682.

X-ray crystallography: Suitable crystals for all four compounds were selected and mounted on a Gemini kappa-geometry diffractometer (Agilent Technologies UK Ltd) equipped with an Atlas CCD detector and using Cu radiation (λ= 1.5418 Å). Intensities were collected at 150 K for *anti*-**5** and *syn*-**6** by means of the CrysalisPro software Reflection indexing, unit-cell parameters refinement, Lorentz-polarization correction, peak integration and background determination were carried out with the CrysalisPro software.[22] An analytical absorption correction was applied using the modeled faces of the crystal.[23] The resulting set of *hkl* was used for structure solution and refinement. The structures were solved by direct methods with SIR97 and the least-square refinement on F^2 was achieved with the CRYSTALS software.[24,25] All non-hydrogen atoms were refined anisotropically. The hydrogen atoms were all located in a difference map, but those attached to carbon atoms were repositioned geometrically. The H atoms were initially refined with soft restraints on the bond lengths and angles to regularize their geometry (C---H in the range 0.93--0.98 Å) and U_{iso}(H) (in the range 1.2-1.5 times U_{eq} of the parent atom), after which the positions were

refined with riding constraints. For compound *anti*-**5**, a chloroform solvent molecule could be located outside the cryptophane cage. Nevertheless this structure contains additional solvent molecules inside the cryptophane cages that could not be localized. The contribution of the disordered solvent molecules was removed using the SQUEEZE algorithm.[26]
CCDC 1525399, 1525400, contains the supplementary crystallographic data for *anti*-**4** and *syn*-**5**, respectively. These data can be obtained free of charge from The Cambridge Crystallographic Data Centre via www.ccdc.cam.ac.uk/data_request/cif.

Laser-Polarized ^{129}Xe NMR spectroscopy: Hyperpolarized xenon was produced through the spin-exchange method in the batch mode using a home built apparatus based on two coupled 30 W laser diodes.[27] Frozen xenon was stored and transported in a glass reservoir immersed in liquid nitrogen. For the transfer to the NMR tube this reservoir was heated and installed in a vacuum line in the fringe field of the NMR magnet. A hollow NMR spinner enabled us to condensate hyperpolarized xenon on top of the solution without freezing the solution.

Acknowledgements

Support from the French Ministry of Research (project ANR-12-BSV5-0003 MAX4US) is greatly acknowledged.

Keywords: Cryptophanes • hyperpolarized xenon • molecular recognition • SPINOE • NMR

[1] a) C. Landon, P. Berthault, F. Vovelle, H. Desvaux, *Protein Science*. **2001**, 762-770. b) L. Dubois, S. Parrès, J. G. Huber, P. Berthault, H. Desvaux, *J. Phys. Chem. B* **2004**, *108*, 767-773.

[2] T. Brotin, J. P. Dutasta, *Chem. Rev.* **2009**, 88-130

[3] M. El Haouaj, M. Luhmer, Y. H. Ko, K. Kim, K. Bartik, *J. Chem. Soc. Perkin. Trans. 2*, **2001**, 804-807.

[4] K. Bartik, M. Luhmer, S. J. Heyes, R. Ottinger, J. Reisse, *Journal of Magnetic Resonance, serie B* **1995**, *109*, 164-168.

[5] K. Bartik, M. Luhmer, J. P. Dutasta, A. Collet, J. Reisse, *J. Am. Chem. Soc.* **1998**, *120*, 784 – 791.

[6] a) L. L. Chapellet, J. R. Cochrane, E. Mari, C. Boutin, P. Berthault, T. Brotin, *J. Org. Chem.* **2015**, *80*, 6143-6151. b) E. Dubost, J. -P. Dognon, B. Rousseau, G. Milanole, C. Dugave, E. Boulard, E. Léonce, C. Boutin, P. Berthault, *Angew. Chem. Int. Ed.* **2014**, *53*, 9837-9840. c) E. Dubost, N. Kotera, S. Garcia-Argote, Y. Boulard, E. Léonce, C. Boutin, P. Berthault, C. Dugave, B. Rousseau, *Org. Lett.* **2013**, *15*, 2866-2868.

[7] a) M. M. Spence, S. Rubin, I. E. Dimitrov, R. J. Ruiz, D. E. Wemmer, A. Pines, S. Q. Yao, F. Tian, P. G. Schultz, *Proc. Natl. Acad. Sci. U.S.A.* **2001**, *98*, 10654-10657. b) L. Schroder, T. J. Lowery, C. Hilty, D. E. Wemmer, A. Pines, *Science*, **2006**, *314*, 446-449. c) T. J. Lowery, S. Garcia, L. Chavez. E. J. Ruiz, T. Wu, T. Brotin, J.-P. Dutasta, D. S. King, P. G. Schultz, A. Pines, A.; D. E. Wemmer, *ChemBioChem* **2006**, *7*, 65-73. d) S. Klippel, J. Dopfert, J. Jayapaul, M. Kunth, F. Rossella, M. Schnurr, C. Witte, C. Freund, L. Schröder, *Angew. Chem. Int. Ed.* **2014**, *126*, 503-506. e) C. Witte, V. Martos, H. M. Rose, S. Reinke, S. Klippel, L. Schröder, C. P. R. Hackenberger, *Angew. Chem. Int. Ed.* **2015**, *54*, 2806-2810. f) N. S. Khan, B. A. Riggle, G. Seward, Y. Bai, I. J. Dmochowski, *Bioconjugate Chem.* **2015**, *26*, 101-109.

[8] T. Brotin, A. Lesage, L. Emsley, A. Collet, A. *J. Am. Chem. Soc.* **2000**, *122*, 1171-1174.

[9] a) C. Boutin, A. Stopin, L. Fatimazorha, T. Brotin, J. P. Dutasta, N. Jamin, A. Sanson, Y. Boulard, F. Leteurtre, G. Huber, A. Bogaert-Buchmann, N. Tassali, H. Desvaux, M. Carriere, P. Berthault. *Bioorganic and Medicinal chemistry* **2011**, *19*, 4135-4143. b) N. Kotera, N. Tassali, E. Léonce, C. Boutin, P. Berthault, T. Brotin, J. P. Dutasta, L. Delacour, D. A. Buisson, F. Taran, S. Coudert, B. Rousseau. *Angew. Chem. Int. Ed.* **2012**, *51*, 4100-4103.

[10] H. A. Fogarty, P. Berthault, T. Brotin, G. Huber, H. Desvaux, J. -P. Dutasta, *J Am. Chem. Soc.* **2007**, *129*, 10332–10333.

[11] R. M. Fairchild, A. I. Joseph, K. T. Holman, H. A. Fogarty, T. Brotin, J. -P. Dutasta, C. Boutin, G. Huber, P. Berthault, *J. Am. Chem. Soc.* **2010**, *132*, 15505-15506.

[12] M. Luhmer, B. Goodson, Y. Q. Song, D.-D. laws, L. Kaiser, M. C. Cyrier, A. Pines, *J. Am. Chem. Soc.*, **1999**, *121*, 3502-3512.

[13] a) N. Daugey, T. Brotin, N. Vanthuyne, D. Cavagnat, T. Buffeteau, *J. Phys. Chem. B* **2014**, *118*, 5211-5217. b) T. Brotin, N. Vanthuyne, D. Cavagnat, L. Ducasse, T. Buffeteau, *J. Org. Chem.* **2014**, *79*, 6028-6036.

[14] E. Dubost, J. -P. Dognon, B. Rousseau, G. Milanole, C. Dugave, Y. Boulard, E. Léonce, C. Boutin, P. Berthault, *Angew. Chem. Int. Ed.* **2014**, *53*, 9837-9840.

[15] T. Brotin; D. Cavagnat, E. Jeanneau, T. Buffeteau, *J. Org. Chem.* **2013**, *78*, 6143 - 6153.

[16] T. Brotin, V. Roy, J. -P. Dutasta, *J. Org. Chem*. **2005**, *70*, 6187 – 6195.

[17] D. Cavagnat, T. Brotin, J.-L. Bruneel, J. P. Dutasta, A. Thozet, M. Perrin, and F. Guillaume, *J. Phys. Chem. B*, **2004**, *108*, 5572-5581.

[18] G. Huber, L. Beguin, H. Desvaux, T. Brotin, H. A. Fogarty, J. -P. Dutasta, P. Berthault, *J. Phys. Chem. A*, **2008**, *112*, 11363 - 11372.

[19] M. Haake, A. Pines, J. A. Reimer, R. Seydoux, *J. Am. Chem. Soc.* **1997**, *119*, 11711-11712.

[20] H. Desvaux, T. Gautier, G. Le Goff, M. Petro, P. Berthault, *Eur. Phys. J. D.* **2000**, *12*, 289-296.

[21] a) M. Kunth, C. Witte, L. Schröder, *J. Chem. Phys.* **2014**, *141,* 194202. b) M. Kunth, C. Witte, A. Hennig, L. Schröder, *Chem. Sci.* **2015***, 6*, 6069–6075. c) S. Korchak, W. Kilian, L. Mitschang, *Chem. Commun.* **2015***, 51*, 1721–1724. d) S. Korchak, W. Kilian, L. Schröder, L. Mitschang, *J. Magn. Reson.* **2016**, *265*, 139–145.

[22] CrysAlisPro, Agilent Technologies, Version 1.171.36.28 (release 20-01-2011 CrysAlis171 .NET) (compiled Feb 1 2013,16:14:44).

[23] R. C. Clark, J. S. Reid, *Acta Cryst. A* **1995**, *51*, 887-897.

[24] A. Altomare, M. C. Burla, M. Camalli, G. L. Cascarano, C. Giacovazzo, A. Guagliardi, A. Grazia, G. Moliterni, G. Polidori, R. J. Spagna, *App. Cryst.* **1999**, *32*, 115-119.

[25] P. W. Betteridge, J. R. Carruthers, R. I. Cooper, K. Prout, D. J. Watkin, *J. Appl. Cryst.* **2003**, *36*, 1487.

[26] P. V. D. Sluis, A. L. Spek, *Acta Cryst. A* **1990**, *46*, 194-201.

[27] C. Chauvin, L. Liagre, C. Boutin, E. Mari, E. Léonce, G. Carret, B. Coltrinari, P. Berthault, *Rev. Sci. Instrum.* **2016**, *87*, 016105.

Supporting Information

Role of the methoxy groups in cryptophanes for complexation of xenon. Conformational Selection Evidenced by ^{129}Xe-^{1}H NMR SPINOE Experiments.

Patrick Berthault, [*b] *Céline Boutin,* [b] *Estelle Léonce,* [b] *Erwann Jeanneau,* [c] *Thierry Brotin*[*a]

[a] Laboratoire de Chimie de l'ENS LYON, UMR 5182 - CNRS, École Normale Supérieure de Lyon, 46 Allée d'Italie, 69364 Lyon, France

[b] NIMBE, CEA, CNRS, Université Paris-Saclay, CEA Saclay 91191 Gif-sur-Yvette, France

[c] Centre de Diffractométrie Henri Longchambon, Université Lyon 1, 5 rue de La Doua, 69100 Villeurbanne, France.

S8: ^{1}H NMR spectra of compounds **9a** (left) and **9s** (right) for the degassed solutions (spectra a and d); in the presence of xenon (spectra b and e). ^{129}Xe-^{1}H SPINOE spectra of compounds **9a** (spectrum c) and **9s** (spectrum f).

S9: ^{1}H NMR spectra of compounds **6a** (left) and **6s** (right) for the degassed solutions (spectra a and d) ; in the presence of xenon (spectra b and e). ^{129}Xe-^{1}H SPINOE spectra of compounds **6a** (spectrum c) and **6s** (spectrum f).

S10: ^{129}Xe NMR spectra of compounds **3a** (left) and **3s** (right) at 293K

S11: ^{1}H NMR spectra of compounds **3a** (left) and **3s** (right) for the degassed solutions (spectra a and d) ; in the presence of xenon (spectra b and e). ^{129}Xe-^{1}H SPINOE spectra of compounds **3a** (spectrum c) and **3s** (spectrum f).

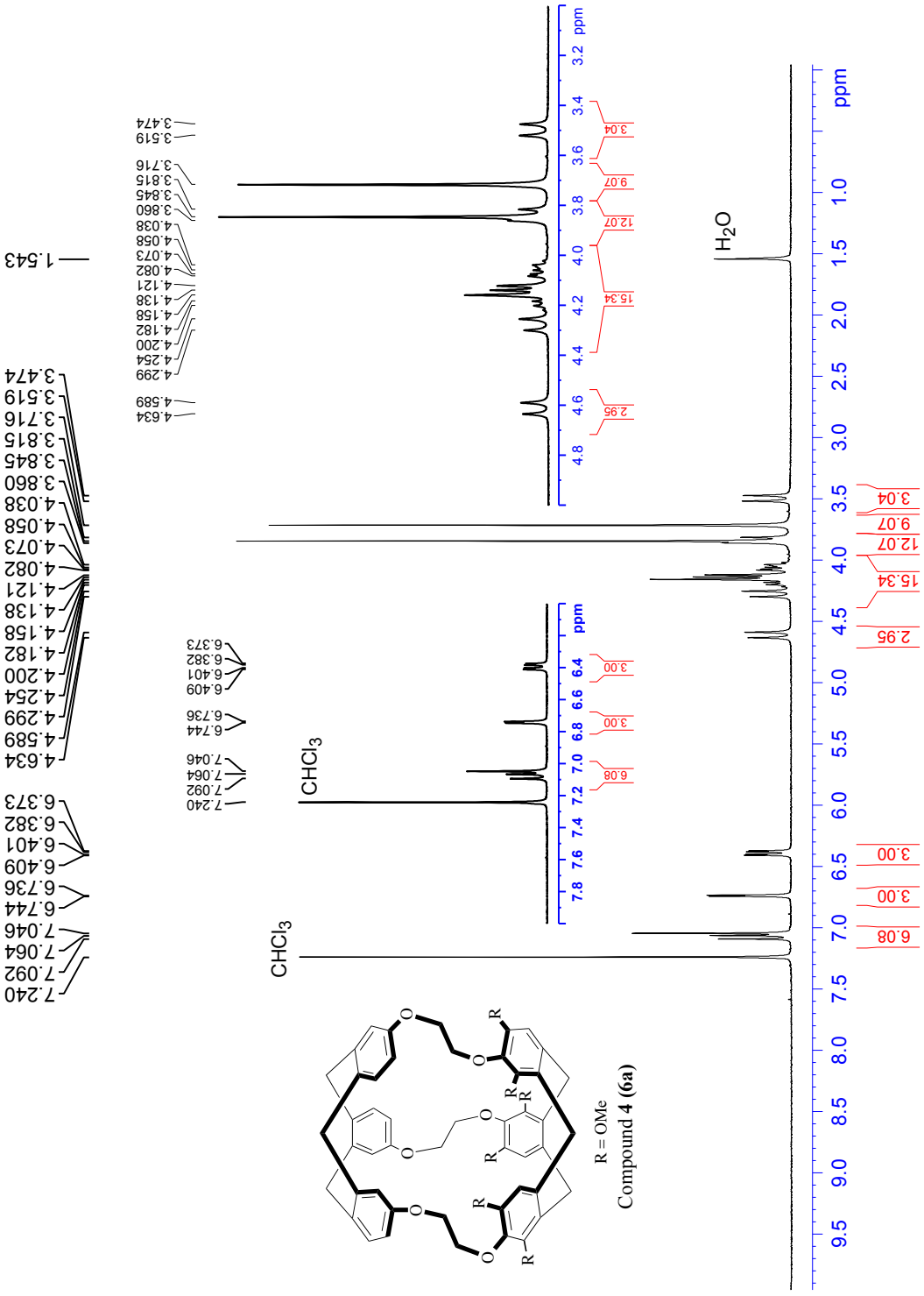

S1 : ^{1}H NMR (300 MHz) spectrum of compound (**4**)-**6s** in $CDCl_3$ solution at 298 K.

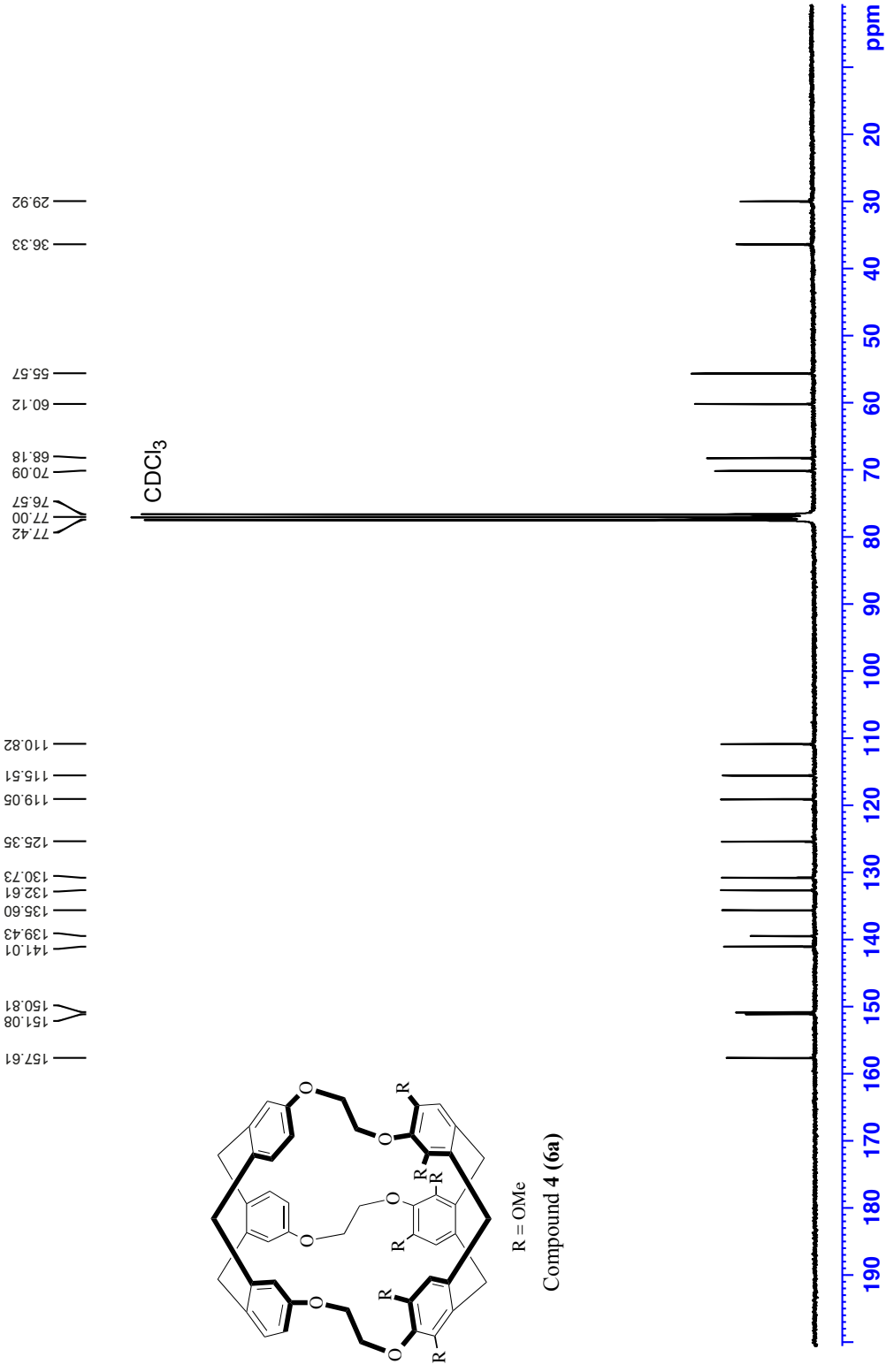

S2 : ^{13}C NMR (75.5 MHz) spectrum of compound (**4**)-**6a** in $CDCl_3$ solution at 298 K.

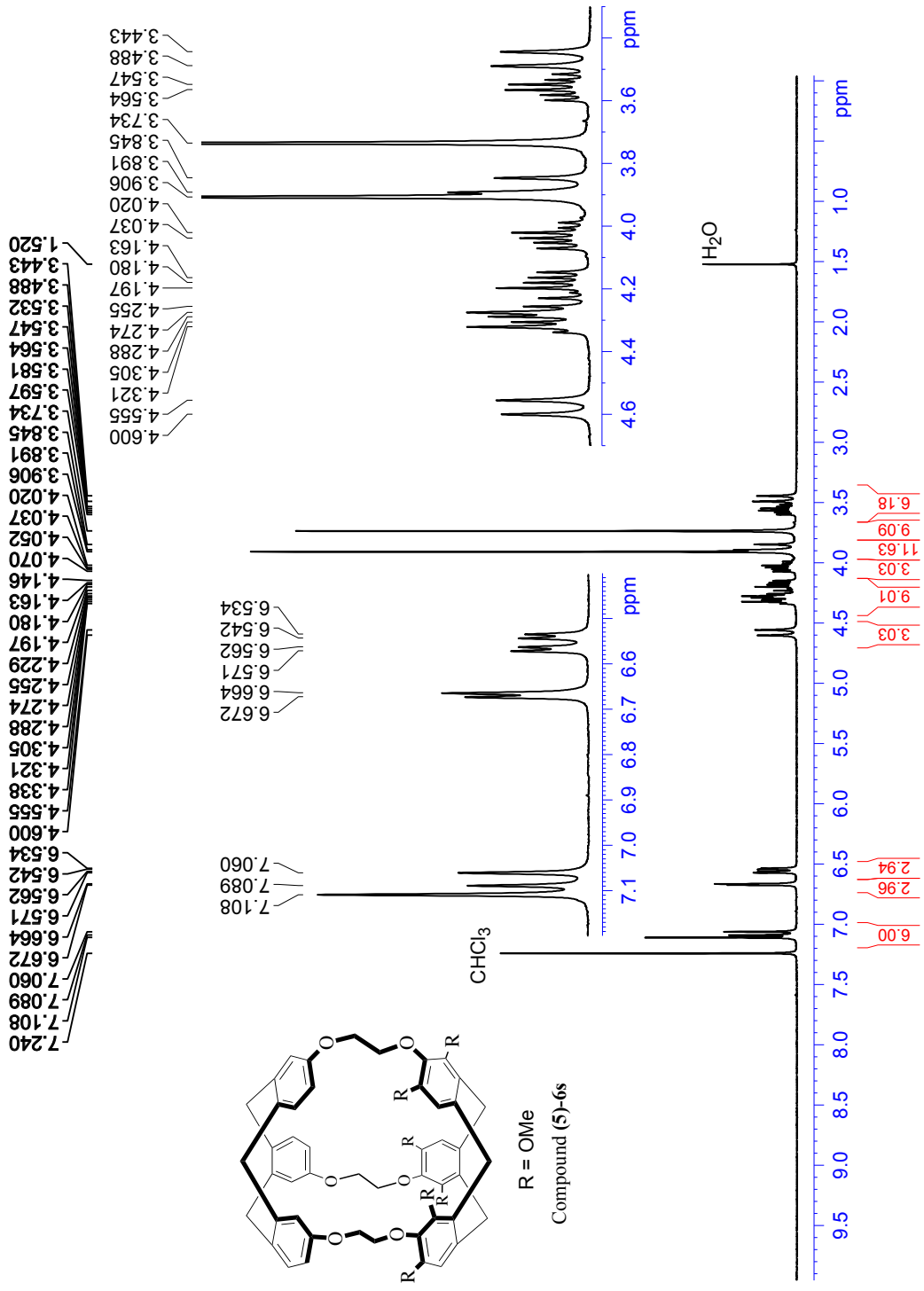

S3 : ^{1}H NMR (300 MHz) spectrum of compound (**5**)-**6s** in $CDCl_3$ solution at 298 K.

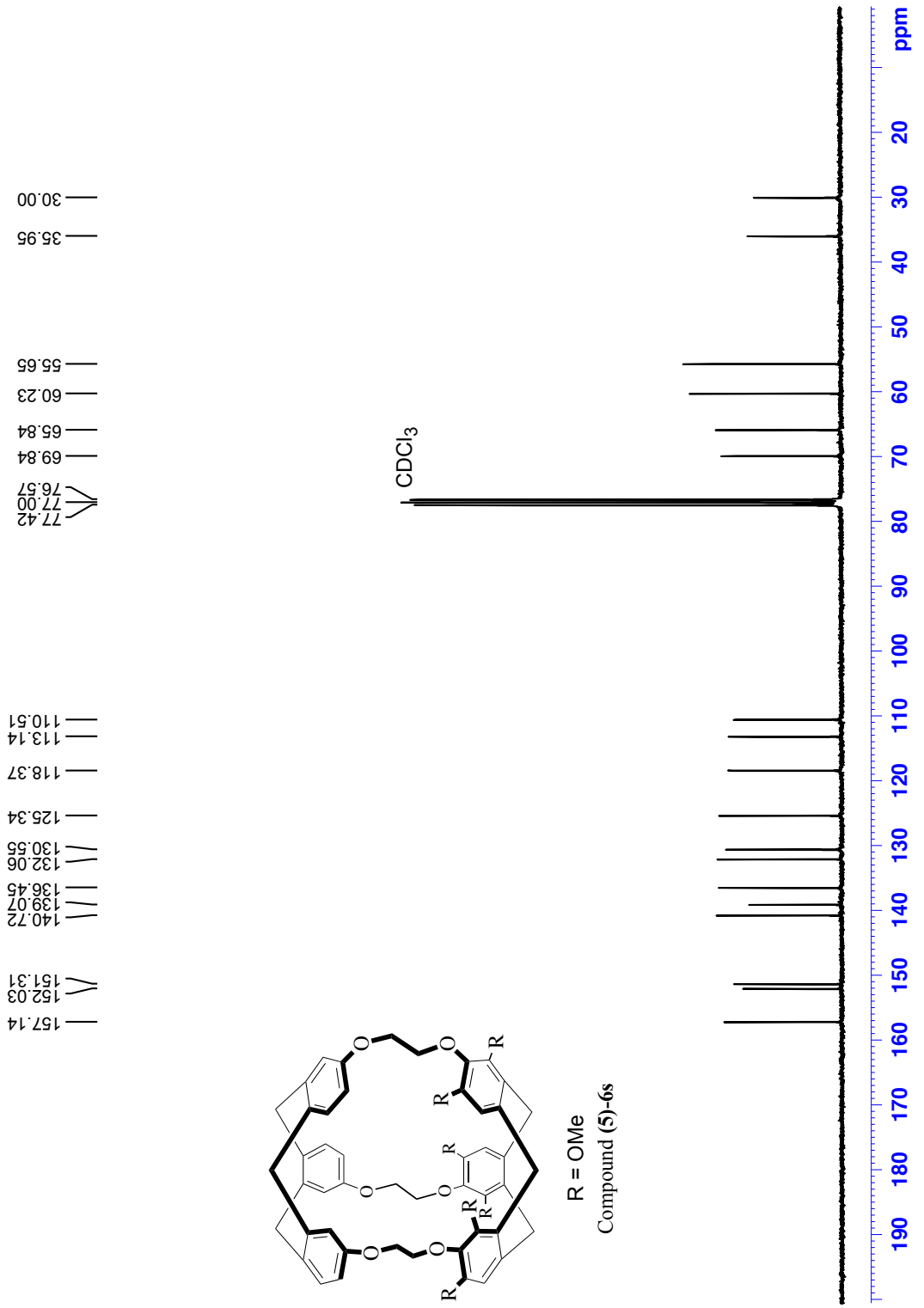

S4 : ^{13}C NMR (75.5 MHz) spectrum of compound (**5**)-**6s** in $CDCl_3$ solution at 298 K.

Table 1: crystallographic data for diastereomers *anti*-**4** and *syn*-**5**

diastereomers	*syn*-**5**	*anti*-**4**
Chemical formula	$C_{54}H_{54}O_{12}\cdot 2(CHCl_3)$	$C_{54}H_{54}O_{12}\cdot CHCl_3$
Molecular weight	1133.77 g.mol^{-1}	1014.39 g.mol^{-1}
Crystal system	Monoclinic	Monoclinic
Space group	$P2_1/n$	$P2_1/n$
Z	2	2
Unit-cell parameters	a = 13.0929 (3) Å b = 22.0159 (4) Å c = 18.1576 (5) Å α = 90 ° β = 93.850 (2)° γ = 90 °	a = 12.3095 (1) Å b = 20.8271(2) Å c = 20.5995 (2) Å α = 90 ° β = 92.3869 (8)° γ = 90 °
Volume	5222.2 (2) Å^3	5276.54 (8) Å^3
R[F^2 > 2σ(F^2)]	0.074	0.048
wR(F^2)	0.158	0.084
GoF	1.06	0.95
Number of reflections (I > 2.0σ(I))	9216	9300
Number parameters	677	650
Number of restraints	921	897
Residual density	-1.27 e Å^{-3} 1.17 e Å^{-3}	-0.79 e Å^{-3} 0.69 e Å^{-3}

S5 : crystallographic data for diastereomers (**4**)-**6a** and (**5**)-**6s**.

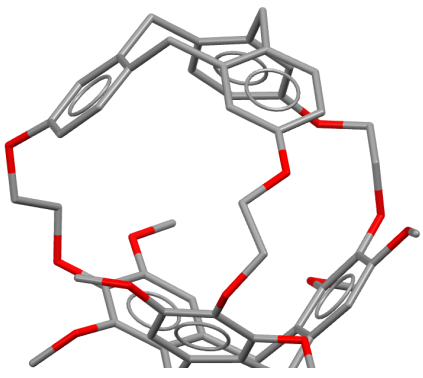

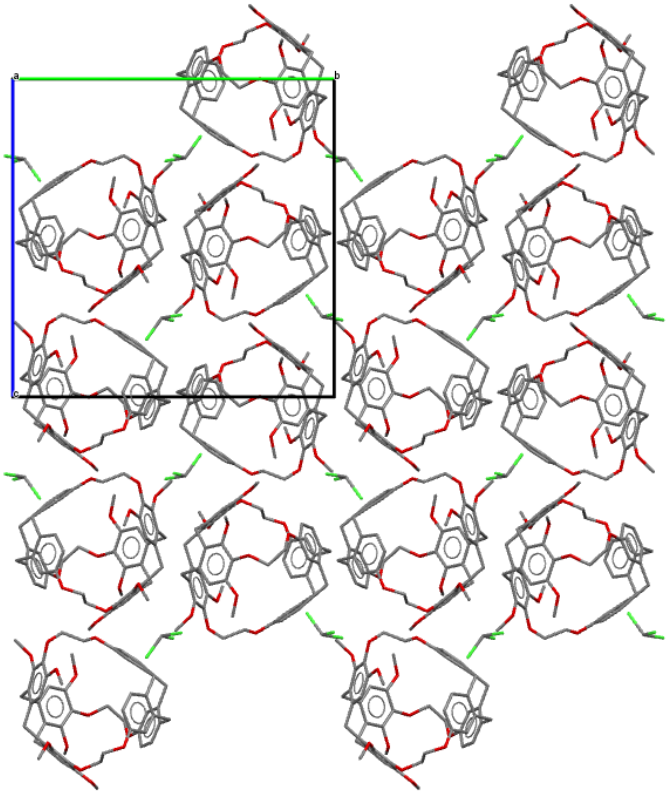

S6 : (top) View of cryptophane (**4)-6a** (hydrogen atoms and disordered parts have been omitted for clarity). (bottom) Projection af the packing of molecule **6** along the **a** unit-cell axis.

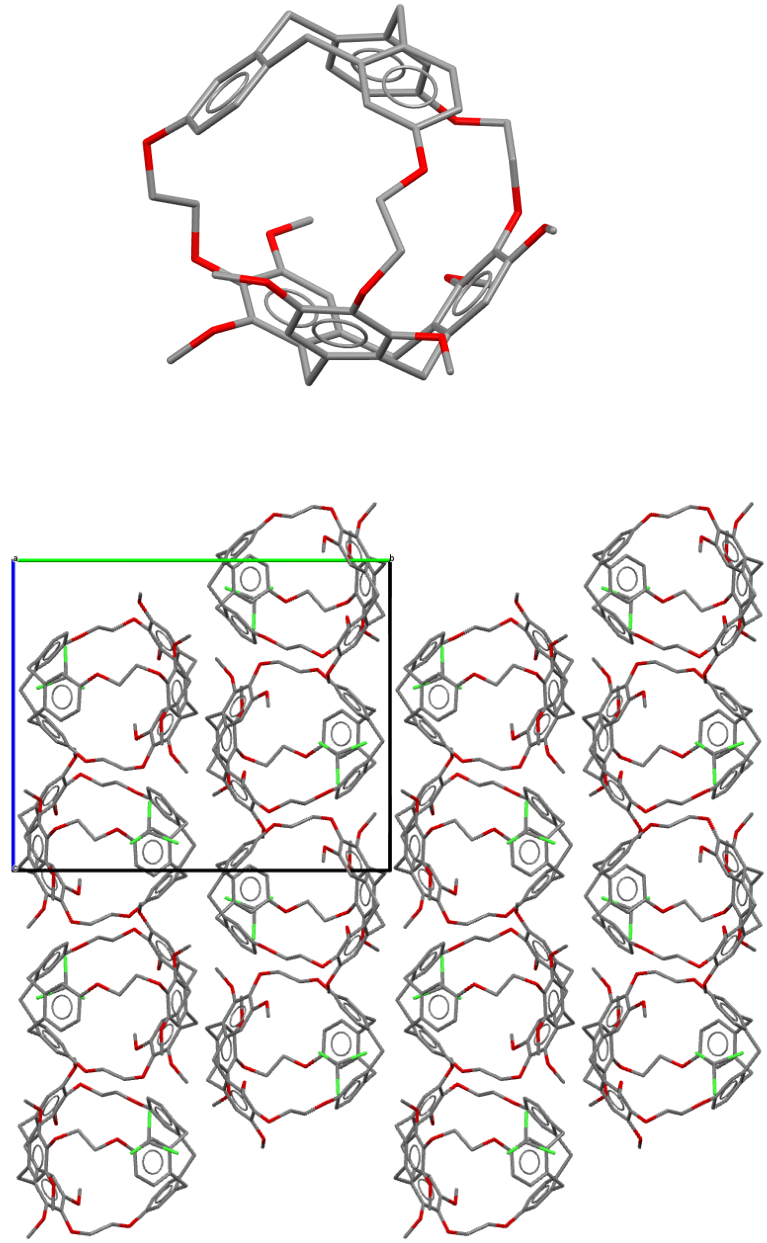

S7 : (top) View of cryptophane (**5)-6s** (hydrogen atoms and disordered parts have been omitted for clarity). (bottom) Projection af the packing of molecule **(5)-6s** along the **a** unit-cell axis.

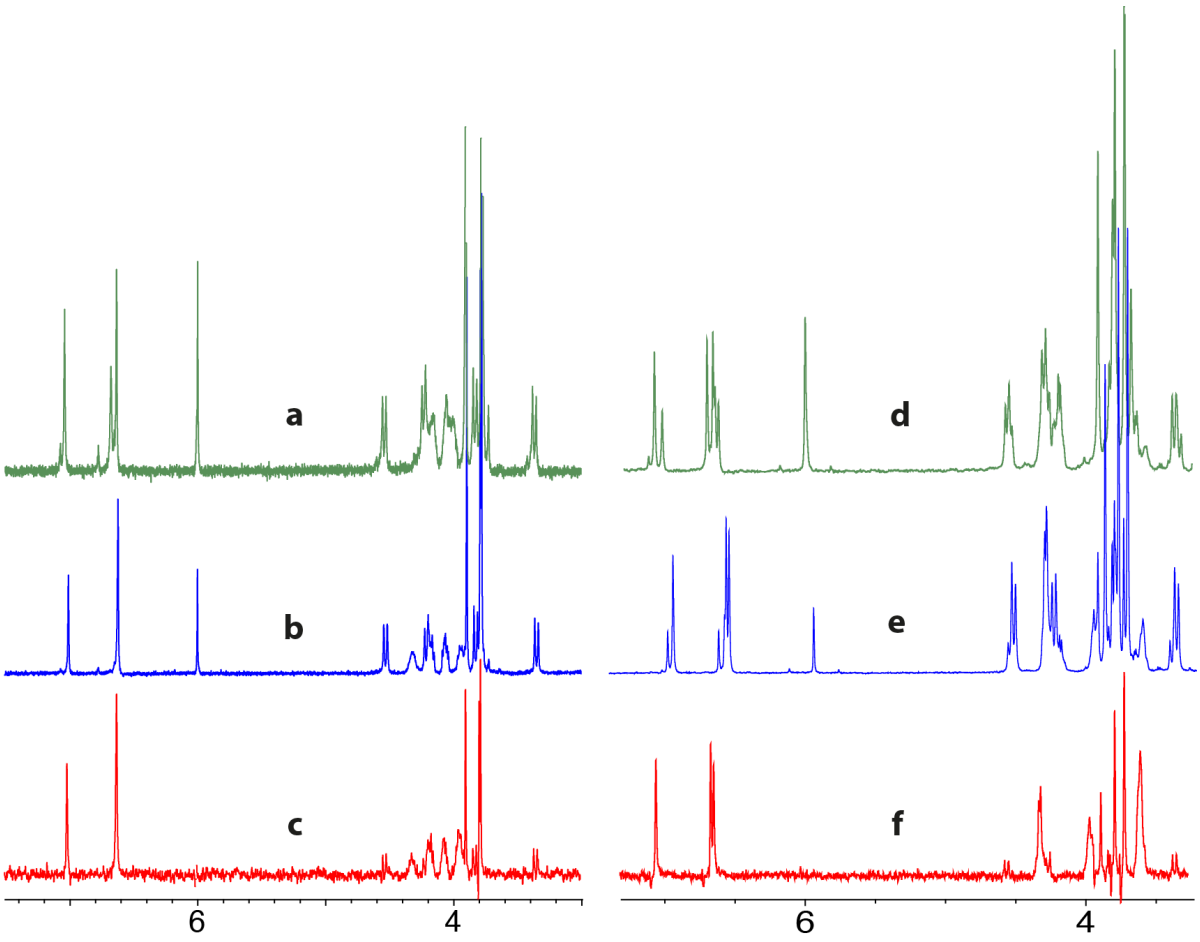

S8 : ^{1}H NMR spectra of compound **9a** (left) and **9s** (right) for the degassed solutions (spectra a and d) ; in presence of xenon (spectra b and e). ^{129}Xe-^{1}H SPINOE spectra of compounds **9a** (spectrum c) and **9s** (spectrum f).

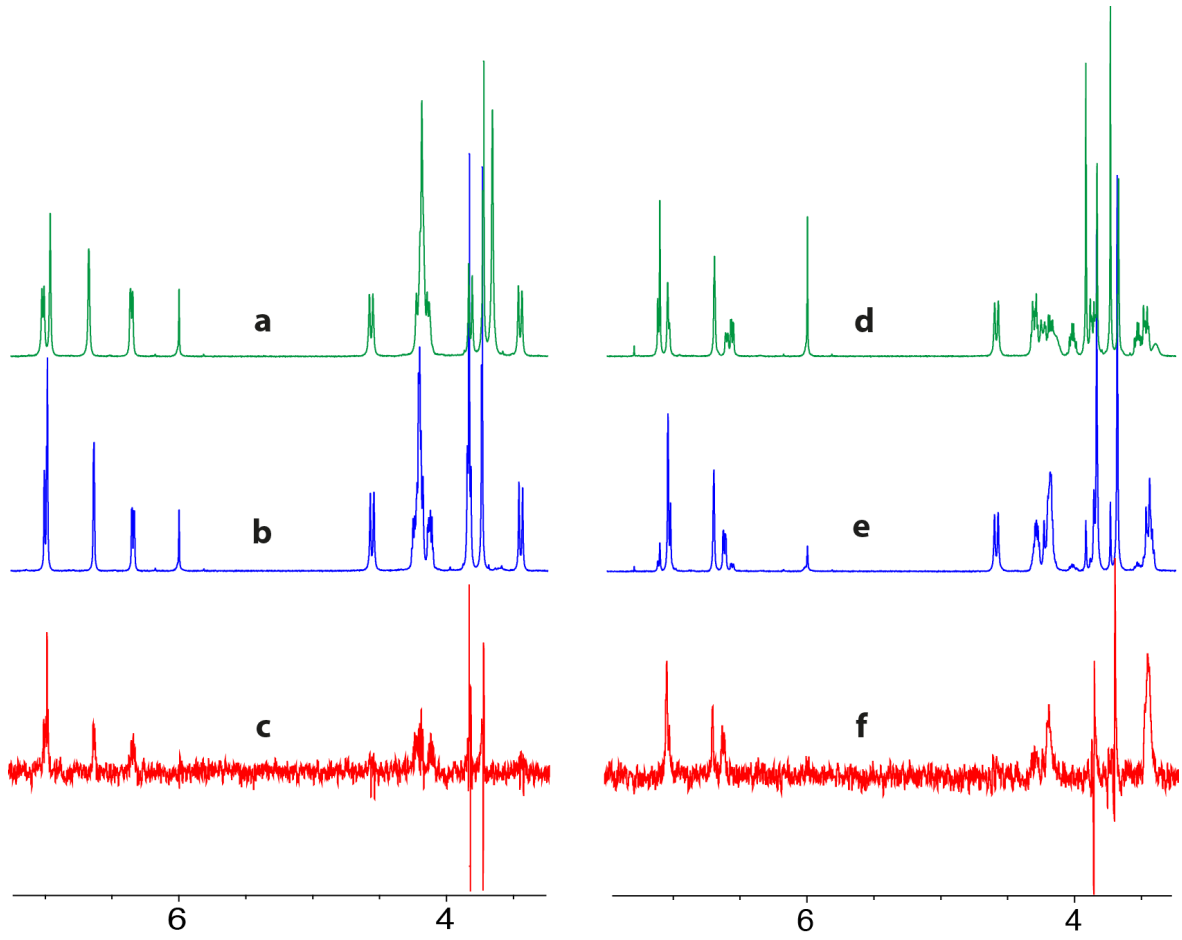

S9 : ^{1}H NMR spectra of compound **6a** (left) and **6s** (right) for the degassed solutions (spectra a and d) ; in the presence of xenon (spectra b and e). ^{129}Xe-^{1}H SPINOE spectra of compounds **6a** (spectrum c) and **6s** (spectrum f). The antiphase signals are not SPINOE, but artefacts due to bad subtraction.

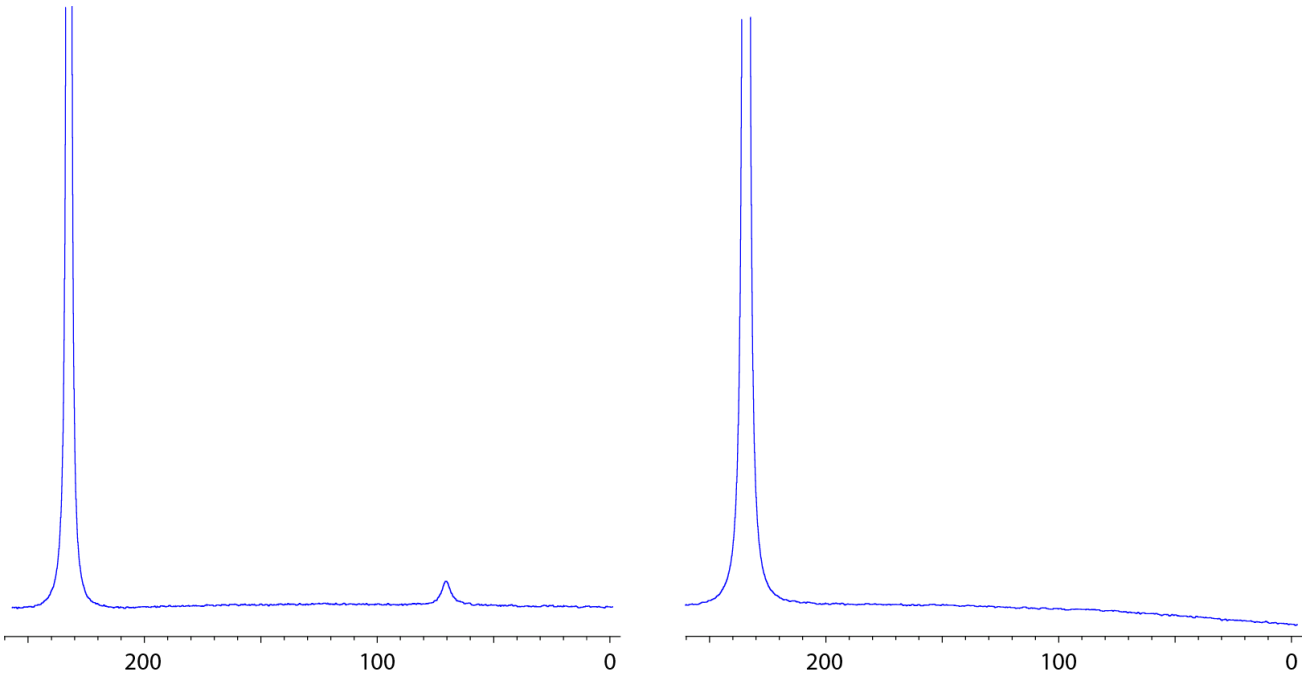

S10: ^{129}Xe NMR spectra of compounds **3a** (left) and **3s** (right) at 293K

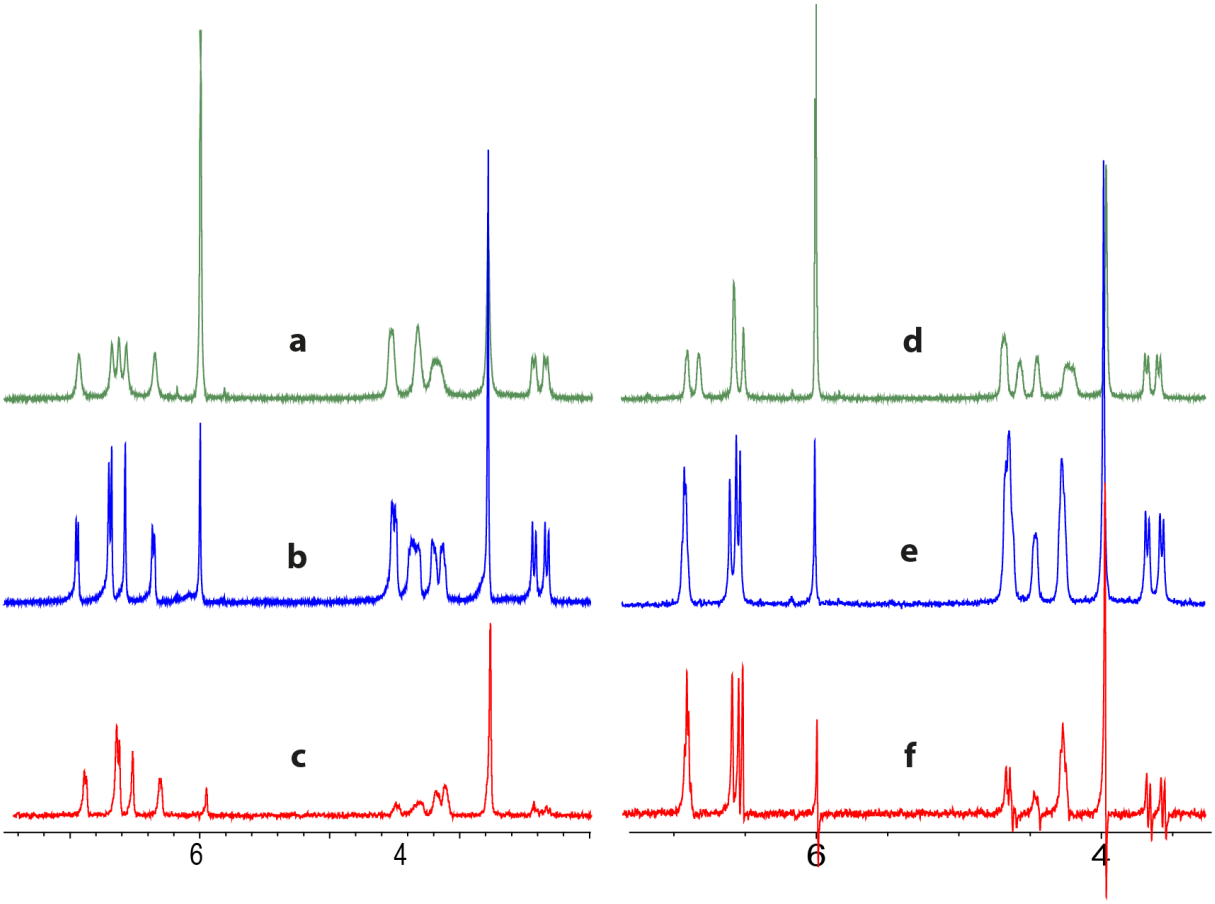

S11: ^{1}H NMR spectra of compounds **3a** (left) and **3s** (right) for the degassed solutions (spectra a and d) ; in the presence of xenon (spectra b and e). ^{129}Xe-^{1}H SPINOE spectra of compounds **3a** (spectrum c) and **3s** (spectrum f). The antiphase signals are not SPINOE, but artefacts due to bad subtraction.